Babeş - Bolyai University
Faculty of Physics

Doctoral Thesis Summary

Fabrication and characterization of new graphene-based nanocomposites with enhanced optical and electronic properties

Maria ILIUȚ

Scientific advisor
Prof. Dr. Simion AȘTILEAN

Cluj – Napoca
2013

Table of Contents

Outline

My thesis is structured in two main parts: **I. Introduction and Background**; **II. Research results and discussions,** and **III. Appendices.**

Part I contains two chapters. **Chapter 1.** ***Graphene Overview*** describes basic aspects related to graphene, namely graphene structure (chemical, crystal and band structure), graphene properties and some related applications. **Chapter 2.** ***Tailoring the properties of graphene*** contains: synthetic methods of graphene and describes in more detail graphene oxide, as building block material of my experiments; the classification of graphene - based composites and some of their applications.

Part II contains four chapters. In **Chapter 3** ***Designing reduced Graphene Oxide – based hybrids for efficient surface Raman scattering (SERS)*** I developed a new green method for the synthesis of graphene – based hybrids, namely reduced graphene oxide – gold nanoparticles (rGO-AuNP) composites, with tunable surface decoration, enables for efficient SERS detection in aqueous environment. **Chapter 4** ***Fluorescence enhancement in highly reduced Graphene Oxide*** studies the interaction of chemically converted graphene species, namely graphene oxide (GO) and reduced graphene oxide (rGO), with a fluorophore – riboflavin (Rb). The study approaches the influence of chemically converted graphene on Rb's fluorescence on one hand, on the other hand, the influence of Rb on GO/rGO's fluorescence is considered. The final goal is the improvement of optical properties in chemically converted graphene, expressed in fluorescence enhancement in rGO. **Chapter 5** ***Fabrication of Graphene Oxide, Carbon Nanotubes and Graphene Oxide – Carbon Nanotubes thin films*** contains the preliminary results of a project, which has as a final goal the fabrication of field effect transistors (FET) on solution based deposited thin films. Here the deposition of single and double – layered graphene oxide films, single walled carbon nanotubes and the combination of both is reported. **Chapter 6** ***Final conclusions and future perspectives*** contains the final conclusions regarding the obtained results and future plans of developing them.

In **III. Appendices** the main spectroscopic techniques used in the experimental part are described.

Keywords: graphene, graphene oxide, reduced graphene oxide, gold nanoparticles, riboflavin, SERS, fluorescence.

I. Introduction and Background

1. Graphene Overview

1.1 Historical background

The first report on graphene, as 2D material, and its electronic properties dates from 2004 *Science* paper of A. Geim and K. Novoselov. In 2010, they won Noble Prize "*for groundbreaking experiments regarding the two-dimensional material graphene".*

1.2 Graphene structure

1.2.1 Chemical bonding and sp^2 hybridization

Carbon atom is the sixth element in the periodic table, having the ground state configuration $1s^2\ 2s^2\ 2p^2$. In graphene the carbon atoms are sp^2 hybridized. Each carbon atom, having three sp^2 hybridized orbitals, forms strong covalent σ (bonding) and σ* (antibonding) bonds with three neighboring atoms, while the remaining p_z orbital, perpendicular on σ bonds, forms π and π* weaker covalent bonds. The bonding orbitals are fully occupied, while the antibonding orbitals are empty.

1.2.2 Crystal structure

The honeycomb graphene lattice is a hexagonal Bravais lattice with a basis of two atoms (A and B). The reciprocal graphene lattice is also hexagonal. The Brillouin zone contains several high – symmetry points: Γ point at the center, the M point – the midpoint of the hexagon, and K point – at the corner of the hexagon. There are six K points and six M points within the first Brillouin zone.

1.2.3 Band structure

Graphene contains two atoms per unit cell. Therefore, it contains eight electronic energy bands given by the six σ and σ*, and the two π and π* levels. These levels arise from eight atomic orbitals per unit cell. The Fermi energy in graphene occurs at zero eV. The valence and conduction bands (π and π* respectively) are degenerate at K points. Therefore, graphene is a zero gap semiconductor (semi – metal). The six K points are equivalent (Dirac points) and the energy at these points has linear dispersion – Dirac cone.

1.3 Some properties of pristine graphene and related applications

Electronic properties: ambipolar electric field effect, ballistic transport, quantum Hall effect at room temperature. *Mechanical properties*: the strongest material ever found (fracture strength of 130 GPa , Young's modulus of 1.0 TPa). *Optical properties:* absorbs ~2.3% of incident light in the whole visible to NIR range; inter- bands (UV-Vis-NIR) and intra - band (far IR) transitions; fast electron – hole recombination – no emission in pristine graphene. *Thermal properties:* superior to any other metal (5000 W m^{-1} K^{-1}). *Surface properties:* high surface specific area - 2600 m^2 g^{-1}.

Properties and related applications are summarized in **Fig. 1-1**.

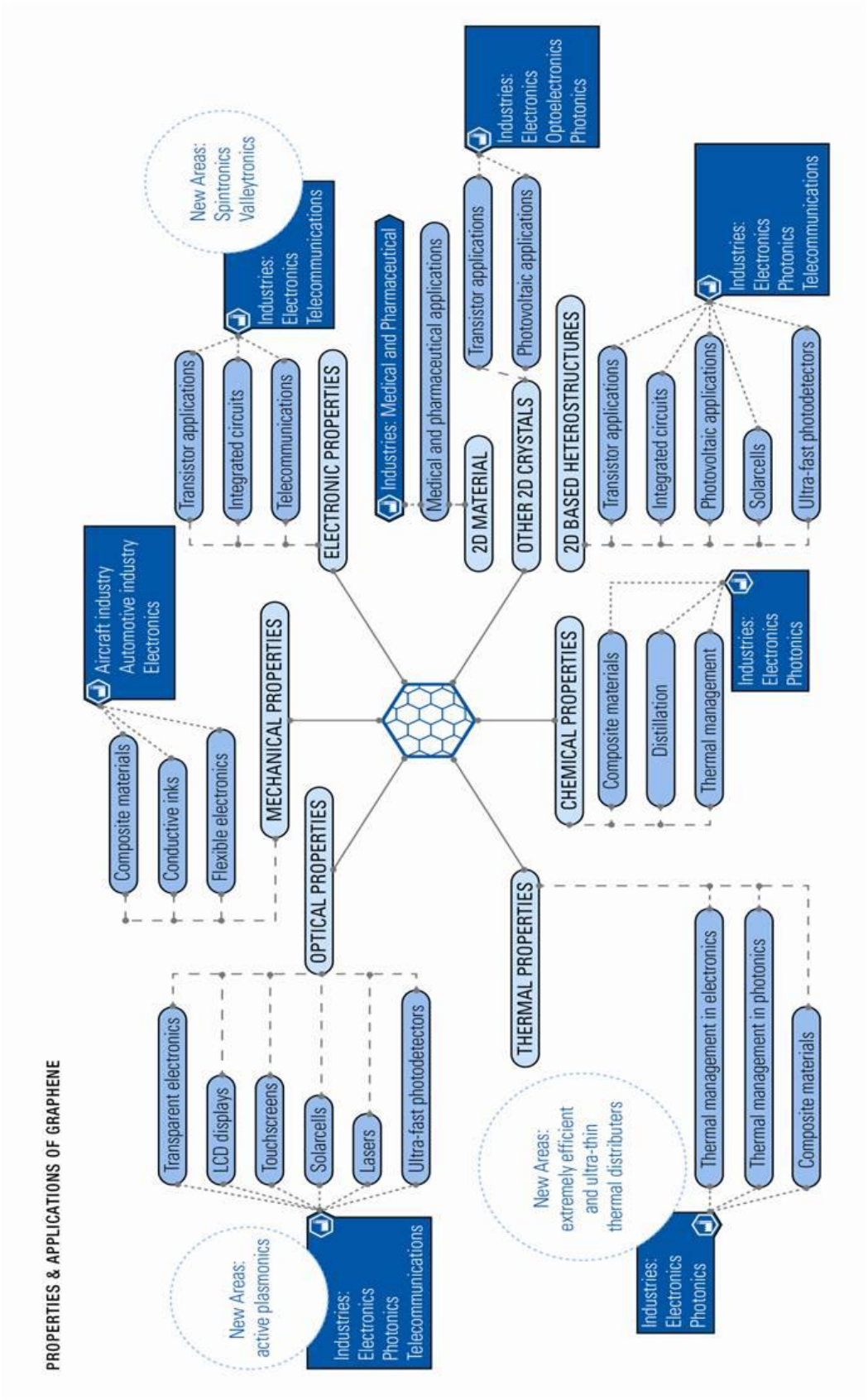

Fig. 1-1 *Graphene properties and related applications. [http://www.graphene-flagship.eu/GF/index.php]*

2. Tailoring the properties of graphene

2.1 Synthetic approaches of graphene

Synthetic approaches comprise two main classes: the top down and bottom up approach, and are summarized in the scheme bellow.

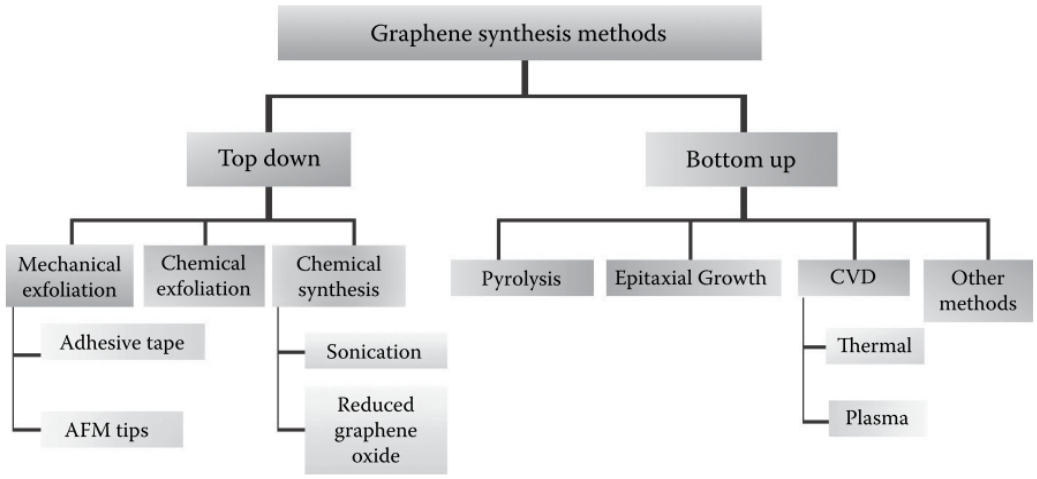

Fig. 2-1 *The schematic representation of the different approaches for graphene synthesis*. [W. Choi and J. Lee, Graphene: synthesis and applications. Boca Raton: CRC Press, 2012]

In this work, chemical synthesis of graphene was used. Therefore, the further focus is on this type of method.

2.2 Chemically converted graphene – graphene oxide

2.2.1 Oxidation mechanism and structural features

The synthesis of graphene oxide, usually performed by Hummers and Offeman method, implies the use of one or more strong acids and an oxidizing agent. The method consists in oxidation of graphite powder, followed by exfoliation by sonication. The resulted graphene oxide is a sheet of graphene having covalently attached hydroxyl, epoxy and carbonil groups on basal planes, and carboxyl and carbonils – at margins, as presented in Fig. 2-2.

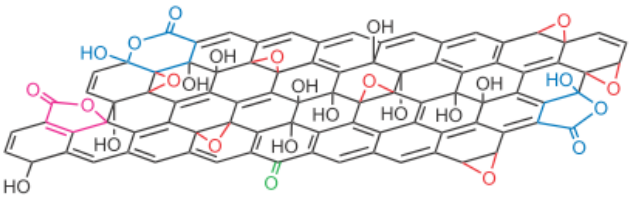

Fig. 2-2 *The structural model of graphene oxide (GO).* [W. Gao, L. B. Alemany, L. Ci, and P. M. Ajayan, "New insights into the structure and reduction of graphite oxide," *Nat. Chem.*, vol. 1, no. 5, pp. 403–408, Aug. 2009]

2.2.2 Morphology

Due to the covalently bonded functional groups on the basal planes and edges, GO presents structural deformation, which determines the apparition of atomic roughness of the sheets, in contrast to sp^2 bonded carbon of the flat graphene. Because of the mixed sp^2-sp^3 structure, GO is an amorphous system with poor or no translational symmetry.

2.2.3 Dispersibility

Due to the various oxygen containing functionalities on the basal plane and margins grafted between aromatic sp^2 domains, GO is considered to have amphiphilic nature with hydrophilic (polar) oxygen groups and hydrophobic (apolar) hexagonal domains. It has good stability in water and several organic solvents.

2.2.4 Reduction

The partial restoration of graphene's properties can be performed by graphene oxide reduction. There are many reduction strategies, classified in thermal, chemical and multi-step reduction.

2.3 Graphene and chemically converted graphene (GO, rGO) – based composites

The functionalization of graphene and its analogues aims the improvement of dispersibility, since graphene is hydrophobic in nature and the processability is very important for many applications. On the other hand, the combination of unique properties of graphene and GO, rGO (*e.g.* conductivity – pristine graphene, mechanical and thermal properties, large surface specific area *etc.*) with those of other components (organic or inorganic reagents) leads to new properties and extent of applicative area.

2.3.1 Graphene/GO/rGO – inorganic nanostructures composites

Since graphene discovery, graphene – inorganic nanostructure composites (*i.e.* metallic and semiconducting nanoparticles) have been extensively studied, due to their tested performances and potential application in catalysis, optics and optoelectronics, supercapacitors, fuel cells, batteries, bio/sensing etc. Inorganic composites refer to metallic nanoparticles such as noble metals: Pt, Au, Ag, Rh and Pd, and semiconducting nanoparticles like: TiO_2, ZnO, SnO_2, MnO_2, Co_3O_4, Fe_3O_4, Fe_2O_3, NiO, Cu_2O, RuO_2, CdS and CdSe. There are many methods of synthesis of graphene – based inorganic nanostructures, divided in two main classes: *ex situ* hybridization and *in situ* crystallization.

2.3.2 Graphene/GO/rGO – polymer composites

Because of the unique properties, including excellent mechanical strength, high surface area, thermal stability and good conductivity, graphene and chemically derived graphene are great candidates to be used as filler material for polymer composites aiming the enhancement of the electronic, mechanical and thermal properties of the polymer. The properties and performances of graphene – polymer composites depends of the quality of graphene, polymer matrix and the bonding between graphene and polymer. Graphene – polymer composites are classified in: *graphene – filled polymer composites, layered graphene – polymer films* and *polymer – functionalized graphene.*

2.3.3 Other graphene/GO/rGO – based composites

Other graphene – based composites can be obtained by functionalization with organic crystals, metal-organic frameworks, biomaterials, carbon nanotubes, fullerenes, fluorophores *etc*.

2.4 Applications of graphene/GO/rGO and graphene/GO/rGO - based composites in bio/sensing, bio-imaging and other biological applications

2.4.1 Bio/Sensing platforms

Field effect transistor (FET) sensors provide the electronic detection of molecules and rely on biorecognition events between the probe and target molecules at the gate of FET. Upon biorecognition the conductivity of the channel between source and drain changes. Because graphene is a zero band gap semiconductor with high surface specific area, and with modulating band gap upon the surface modification, it is an ideal candidate for FET bio/sensors.

Electrochemical Bio/Sensors. Electrochemical detection is highly sensitive to electroactive molecules. It offers the advantages of being sensitive and selective due to the properties of different electroactive molecules to be oxidized or reduced at certain potential. Graphene showed to be great candidate for electrochemical sensing due to excellent electronic properties, sp^2 structure and edges defects that facilitates electron transfer between graphene and molecule, and high surface specific area that enables large amount of electroactive sites.

Fluorescence sensors. Fluorescence – based detection is highly sensitive, selective, rapid and cost – effective for the analysis and bio - detection. The strategy of graphene – based fluorescence sensing consists of graphene's (and rGO/GO) capability to play as great fluorescence quencher due to the resonance energy transfer (RET). Another strategy used in graphene – based fluorescence sensing is based on the photoluminiscent properties of chemically converted graphene – GO and rGO.

SERS (Surface Enhancement Raman Scattering) sensors. Due to the combination of ultrahigh sensitivity with chemical selectivity, SERS technique have been widely implemented by scientific community for chemical and biological measurements, providing the opportunity for the development of ultrasensitive analytical methods for bio/detection. Graphene based SERS rely on fluorescence quenching effect due to the RET and chemical enhancement mechanism. Functionalization of graphene with noble metals leads to a superior SERS performance due to the combination of chemical and electromagnetic mechanisms.

2.4.2 Bio – imaging and other biological applications

Bio – imaging is based on fluorescence properties of GO/rGO, on one hand. On the other hand, due to the high surface specific area, graphene is able to transport fluorescent species (e.g. quantum dots). Other potential applications include photothermal therapy, based on the absorption in NIR of graphene.

II. Research results and Discussions

3. Designing reduced Graphene Oxide – based hybrids for efficient Surface Enhanced Raman Scattering (SERS)

Abstract

In this chapter, a new in situ approach for the synthesis of reduced graphene oxide – gold nanoparticles (rGO – AuNP) hybrids is reported. The prepared hybrids present high stability in aqueous solution due to the use of PVP as stabilizing agent. Moreover, the synthetic process uses only non- toxic reagents, namely ascorbic acid for simultaneous graphene oxide (GO) and Au ions reduction, and PVP is non- toxic polymer used for medical purposes. The synthesis approach was systematically studied and, by changing the reaction parameters, I found that the hybrids' characteristics and properties could be tuned. For instance, it is showed that the reaction temperature can influence the shape of the synthesized AuNP and slightly affects their density. Additionally, the GO surface modification (the reduced and unreduced form) prior to AuNP formation represents an important aspect in hybrids designing. Particularly, when rGO is used as platform for Au ions nucleation, a relative sparse distribution of AuNP is noticed. In contrast, when Au source is added prior to GO reduction, densely and uniformly packed small sized AuNP (3-12 nm) mainly decorate graphene. The results highlight the role of oxygen moieties in AuNPs anchoring onto graphenic surface. Furthermore, the Au ions reduction on unreduced GO relies on the catalytic abilities of AuNP in GO reduction. Finally, the obtained hybrids were employed as SERS substrate for the detection of Nile Blue A and 4mercaptobenzoic acid in liquid environment, and their performance increase with AuNP density on rGO surface and affinity of the analyte molecule to bind to graphene.

3.1 Materials and methods

3.1.1 Chemicals

Graphene oxide synthesis: Graphite powder 99.9995 %, potassium permanganate ($KMnO_4$) 99%, sodium nitrate ($NaNO_3$) 99%, sulphuric acid (H_2SO_4) 96%, hydrogen peroxide (H_2O_2) 30%, hydrochloric acid (HCl) 35%; *stabilization*: polyvinylpyrrolidone (PVP) (MW, 10 kg mol^{-1}); *GO and Au reduction*: L-ascorbic acid (AA) 99%; *Au source*: gold (III) chloride trihydrate ($HAuCl_4 \cdot 3H_2O$) 99.9 %; *SERS experiment*: Nile Blue A (NBA), 4mercaptobenzoic acid (4MBA).

3.1.2 Preparation of graphene oxide (GO)

Graphene oxide (GO) was synthesized according to Hummers and Offeman's method. Briefly, graphite powder was oxidized in the presence of H_2SO_4, $NaNO_3$ and $KMnO_4$. Oxidized graphite was washed with HCl, H_2O_2 and warm distilled water, followed by exfoliation induced by sonication.

3.1.3 Preparation of polyvinylpyrrolydone capped GO (GO – PVP)

GO – PVP was prepared by simply mixing and heating of GO with PVP for 24 h. The excess of PVP was removed by centrifugation.

3.1.4 Preparation of reduced graphene oxide- Au nanoparticles (rGO-AuNP) hybrids

Preparation of S1, S2: GO-PVP was reduced 3 hours in the presence of AA by heating; then Au ions source was added in the hot (S1) and ice-cold (S2) solutions respectively.

Preparation of S3, S4: GO-PVP was first mixed with Au ions source, followed by addition of reducing agent (AA) in the hot (S3) and ice – cold (S4) solutions.

The schematic representation of the synthetic steps is given in **Scheme 3-1**.

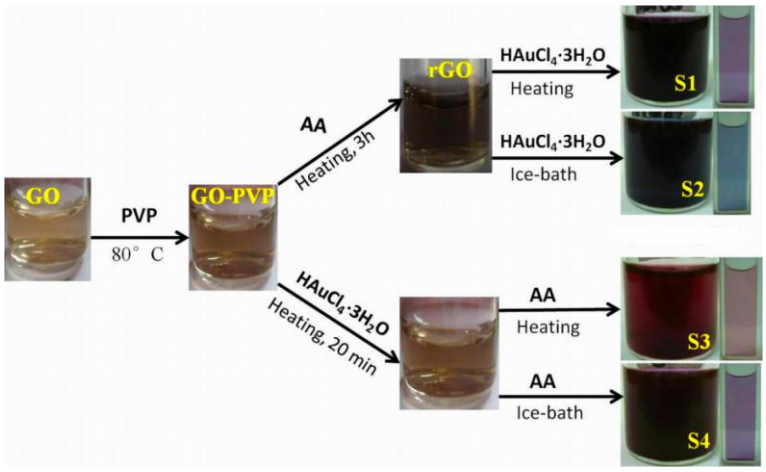

Scheme 3-1 *The schematic illustration of the steps for the synthesis of the rGO-AuNPs hybrids*

3.2 Characterization techniques

For sample characterization, the following techniques were used: UV – Vis spectroscopy, transmission electron microscopy (TEM), atomic force microscopy (AFM), Fourier – transform infrared spectroscopy (FTIR), X- ray diffraction (XRD), X-ray Photoelectron Spectroscopy (XPS), Zeta potential measurements, Raman spectroscopy.

3.3 Characterization of rGO – AuNP hybrids

UV-Vis spectroscopy GO absorption spectrum is characterized by two bands assessed to π-π* (C=C) and n-π* (C=O) transitions. In rGO – AuNP hybrids the C=C band is red shifted due to the reduction of GO, and new bands in Vis range appear, assessed to plasmonic bands in of nano-gold.

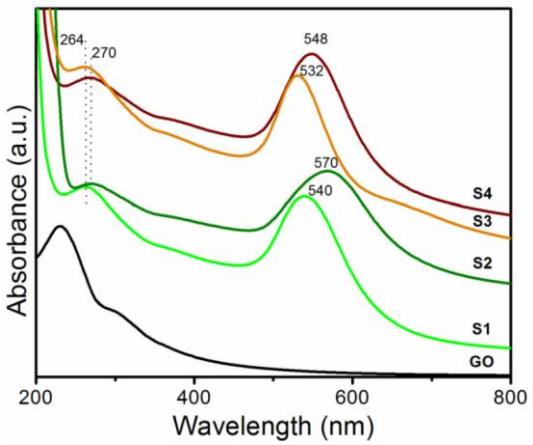

Fig. 3-2 *UV-Vis absorption spectra of GO and rGO-AuNP hybrids.*

TEM (Transmission Electron Microscopy). The successful loading of AuNP on graphene sheets is further confirmed by *TEM*, **Fig. 3-3**.

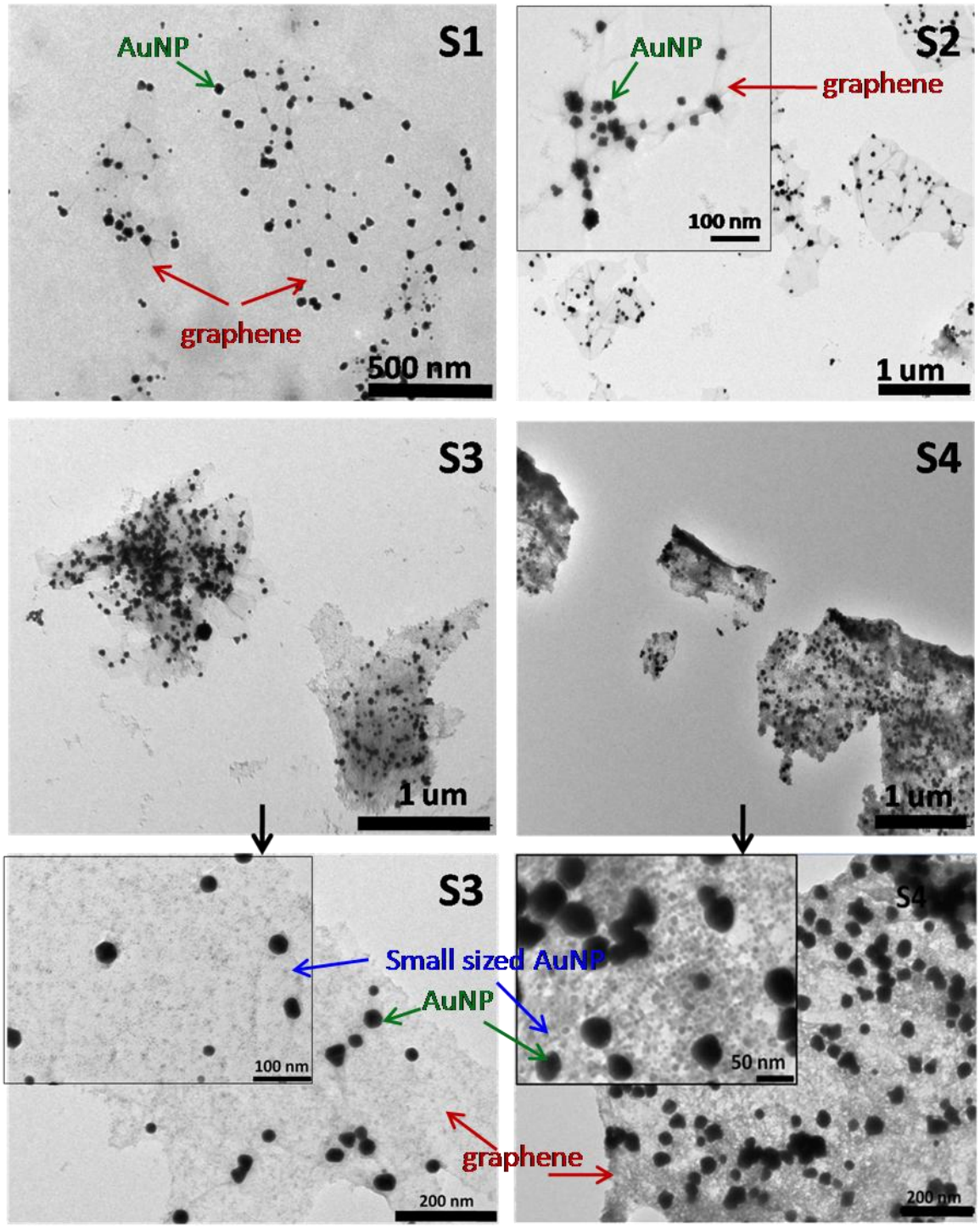

Fig. 3-3 *TEM images of rGO – AuNP hybrids: S1, S2, S3, S4*

AFM is the most appropriate method to study the thickness and surface roughness of graphene and graphene-based composites. AFM shows 1 nm thickness for GO, ~2.5 nm – for GO – PVP, confirming the loading of PVP, and variable sheets thickness in case of rGO – AuNP hybrids, due to the wrinkles produced due to the AuNP anchoring on rGO.

FT-IR spectroscopy was employed to confirm the presence of oxygenated moieties on GO surface, the successful attachment of PVP, as well as GO reduction in all rGO-AuNP hybrid samples. The most prominent peaks of GO spectrum are ascribed to the vibration of oxygen containing groups, while in rGO – AuNP hybrids these vibrations are weakly present due to the reduction of GO.

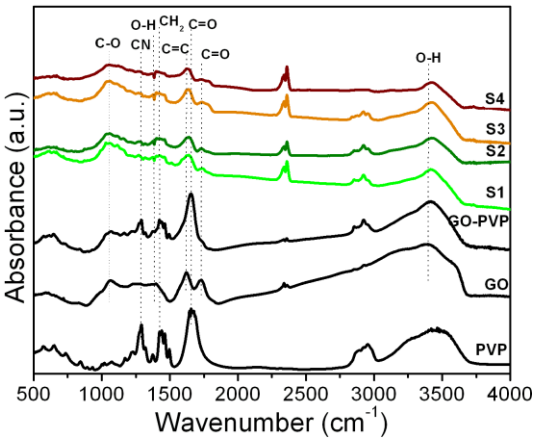

Fig. 3-4 *FT-IR spectra of solid PVP, GO, GO-PVP and rGO-AuNP hybrids.*

XRD is an effective technique for studying the interlayer modifications induced in graphite related materials. Graphite is characterized by an interlayer distance d_{002} = 3.4 Å, while in GO the distance increases to 7.6 Å due to oxygenation, exfoliation and water adsorption. In rGO – AuNP hybrids the carbon interlayer distance decrease relative to GO to ~ 4 Å, due to the reduction and layers stacking. New peaks characteristic to Au *fcc* appears, as an evidence of crystallinity of formed AuNP.

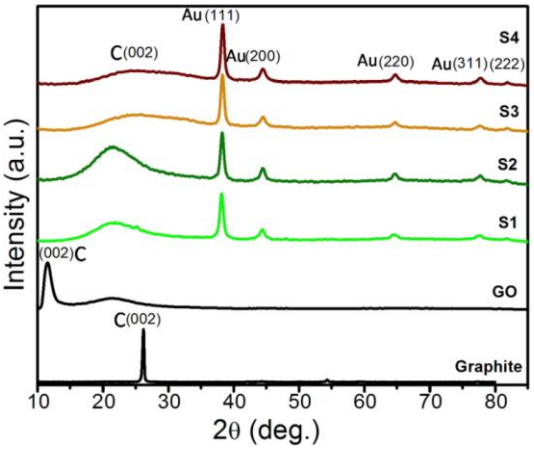

Fig. 3-5 *XRD diffraction patterns of graphite, GO, rGO and rGO-AuNP hybrids.*

XPS measurements (**Fig. 3-6**) reveal the nature of carbon bonds their evolution upon rGO-AuNP hybrids formation. The C1s spectra show an increase of sp^2 carbon from ~20 % in GO to ~ 50 % in rGO involved in rGO – AuNPs hybrids. This rely on reduction of GO during hybrids formation.

Zeta potential measurements show negative potential for rGO – AuNPs hybrids of ~ - 25 mV, whose stability was increased by adding several droplets of ammonia solution (~ - 34 mV).

Zeta potential (mV)									
GO	GO-PVP	Before NH_3 addition				After NH_3 addition			
		S1	S2	S3	S4	S1	S2	S3	S4
-40,2	-26,5	-23,2	-22,5	-27,6	-26,6	-33,8	-31,6	-32,9	-32,9

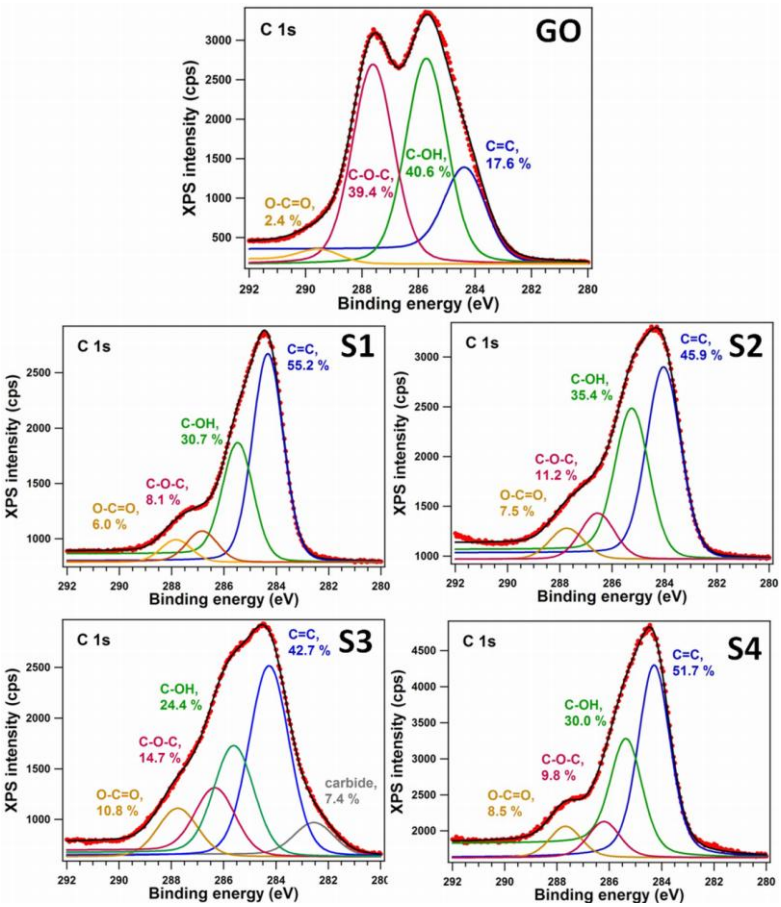

Fig. 3-6 *High resolution C 1s XPS spectra of GO and S1, S2, S3 and S4. Experimental data are red dots, the total fit is the full black curve, while curves with different colors represent individual components.*

<u>*Raman spectroscopy*</u> is a powerful tool widely used for the characterization of graphitic materials in terms of electrons and phonons behavior, providing information about lattice defects and number of graphene layers. GO is characterized by D and G bands, associated with out of plane and in plane vibrations of C=C respectively. The bands shifts indicate on certain type of doping, while the increase in band ratio is associated with reduction and increased number of defects.

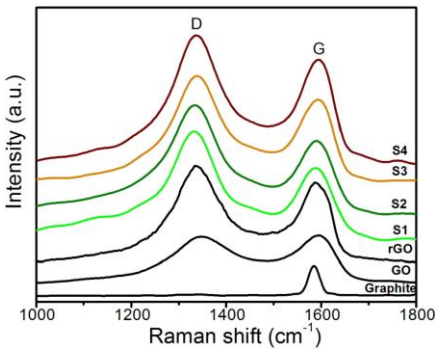

Samples	D band (cm^{-1})	G band (cm^{-1})	I_D/I_G
GO	1348	1598	0.94
rGO	1336	1586	1.22
S1	1333	1589	1.70
S2	1335	1593	1.66
S3	1339	1597	1.39
S4	1338	1596	1.33

Fig. 3-7 *Raman spectra of graphite, GO, rGO and rGO – AuNP hybrids; the corresponding bands position and ratio.*

3.4 Discussions

Comparable degrees of reduction of GO in all rGO-AuNP hybrids rely on catalytic abilities of AuNP in GO reduction.

AuNP density and distribution on rGO surface. The oxygen groups on GO surface play as nucleation sites for AuNP formation. This explains the low density of AuNP in case of S1, S2, where Au nucleation took place on reduced form of GO (low density of oxygen groups); and high density of AuNP in case of S3 and S4, where the Au nucleation occurred on unreduced GO (high density of oxygen groups).

3.5 The efficiency of rGO - AuNP hybrids in SERS detection

The SERS efficiency of as prepared rGO – AuNP hybrids was tested on two different pobe molecules: Nile Blue A (NBA) and 4-mercaptobenzoic acid (4MBA), with higher (ππ stacking) and lower affinity respectively for graphene (**Fig. 3-8**).

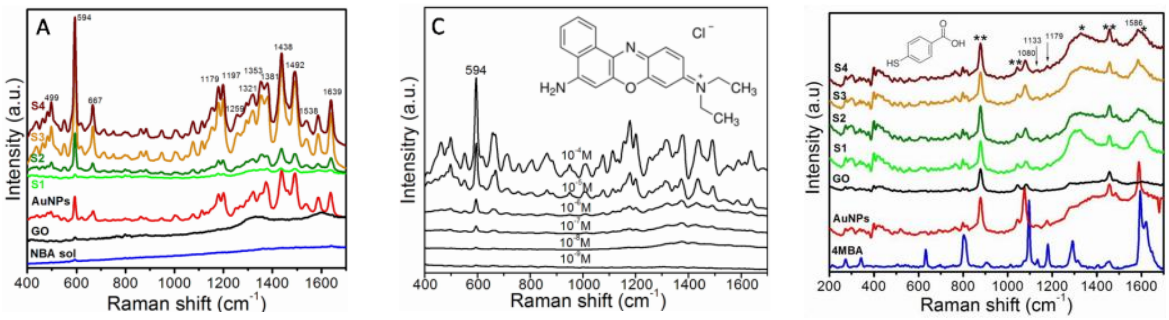

Fig. 3-8 *(left) Raman spectra of 10^{-4} M NBA solution (blue line) and SERS spectra of NBA (10^{-4} M) in GO (black line), Au colloid (AuNP-red line) and rGO-AuPNs hybrids solutions (S1, S2, S3, S4) recorded at 785 nm excitation wavelength, the same laser power and integration time; (middle) SERS spectra of NBA in S4 solution at different concentrations of NBA, in the range of 10^{-4}-10^{-9}M; the inset shows the chemical structure of NBA molecule; (right) Raman spectrum of solid 4MBA (A-blue line) and SERS spectra of 4MBA (10^{-4}M) in AuNP colloid solution (red line), GO sol (black line) and rGO-AuPNs hybrids solution: S1 (green line), S2 (olive line), S3 (orange line), S4 (wine line) taken at 785 nm excitation wavelength. The (*) and (**) denotes rGOs and ethanol peaks respectively. Inset shows the chemical structure of 4MBA molecule.*

The good performance observed in the case of blank Au colloid is due to the aggregation, while no aggregation was observed for any of rGO – AuNP hybrids. Several factors were found to influence the SERS sensitivity of rGO – AuNPs platforms: chemical and electromagnetic mechanisms and the number of molecules in close vicinity to the SERS

substrate. Therefore, the SERS performance of hybrids increased with the density of AuNP on rGO surface and affinity of the probe molecule for SERS substrate. The SERS sensitivity of S4 hybrid was found to be very high, reaching the detection limit for NBA at the concentration of 10^{-9} M in liquid environment.

3.6 Conclusions

- I developed a new, green and easy approach for the synthesis of aqueous stable reduced graphene oxide – Au nanoparticles composites;
- By changing the reactions parameters I found that the sizes and densities of AuNP obtained onto rGO are highly sensitive to the chemistry of chemically converted graphenes' surface prior to the Au ions source addition;
- The systematic study of the reaction conditions allowed the designing of various type of hybrids with different SERS sensing performances;
- The developed synthetic approach is promising in further designing of SERS platforms for bio/sensing studies.

4. Fluorescence enhancement in highly reduced Graphene Oxide

Abstract

Chemically converted graphene, graphene oxide (GO) and reduced graphene oxide (rGO), possesses intrinsic fluorescence, which can be tuned by varying sp^2/sp^3 ratio. However, the fluorescence quantum yield is low and sensitive to environment, limiting its optical applications. In this chapter, I developed a new route towards the improvement of the fluorescence in highly reduced graphene oxide (rGO) through non-covalent interaction with a biological molecule, namely the riboflavin (Rb), a fluorescent micronutrient of the utmost importance in a variety of cellular processes, with a key role in energy metabolism. On the other hand, the interaction of rGO with Rb leads to the fluorescence quenching of the latter. Therefore, rGO-Rb composite can take advantage from both: the improved optical properties of rGO (for e.g. imaging) and the quenched fluorescence of the fluorophore (for e.g. bio/sensing).

4.1 Materials and methods

4.1.1 Chemicals

For the *preparation of GO* – the same previously reminded; *GO reduction*: hydrazine hydrate ($NH_2NH_2 \cdot H_2O$) 24-26% in H_2O (RT); riboflavin (Rb) ($C_{17}H_{20}N_4O_6$, 98%).

4.1.2 Preparation of graphene oxide (GO)

Graphite oxide was synthesized according to Hummers and Offeman's method, described in the previous chapter.

4.1.3 Reduction of GO

The reduction of GO in rGO was performed at 100˚ C in microwaves, by using hydrazine hydrate as reducing agent.

4.1.4 Samples preparation: graphene oxide – riboflavin (GO- Rb), reduced graphene oxide – riboflavin (rGO- Rb).

For monitoring the GO/rGO - Rb induced fluorescence quenching different volumes of GO/rGO were mixed with Rb to keep constant the final concentration of Rb, while chancing the concentration of GO/rGO.

For monitoring the GO/rGO-Rb interaction and Rb induced fluorescence changes in GO/rGO the above prepared solutions were filtered (rGO-Rb) or centrifugated (GO-Rb) and supernatant was further used (*e.g.* the filtering allows the relative removal of Rb excess and of a part of rGO from observation, for avoiding the reabsorption effect during fluorescence measurements).

4.2 Characterization techniques

UV-Vis absorption spectroscopy, steady state and time resolved fluorescence, Raman, AFM, FTIR, XPS, Zeta potential measurements, fluorescence and fluorescence lifetime imaging.

4.3 Characterization and structural analysis of graphene oxide and reduced graphene oxide

This subsection aims the characterization of the precursor materials, GO and rGO, and the monitorization of the degree of reduction in rGO. All used techniques rely on extensive reduction of GO: e.g. XPS spectra show an increase of sp^2 carbon from 50 (GO) to 80 % in rGO.

4.4 Investigation of the interaction between graphene oxide and reduced graphene oxide with riboflavin

4.4.1 Monitoring the graphene oxide and reduced graphene oxide - induced fluorescence quenching in riboflavin

Steady–state and time-resolved fluorescence (TRF) measurements

Fluorescence spectra of Rb-GO/rGO mixtures, at different GO/rGO concentrations, excited at 445 nm (optimum absorption for Rb) show a maximum emission at 530 nm, characteristic to Rb. The intensity of Rb's fluorescence spectra slightly decrease with increase in GO concentration, while in the case of rGO the fluorescence of Rb disappears. This relies on excellent quenching abilities of rGO, as compared to GO.

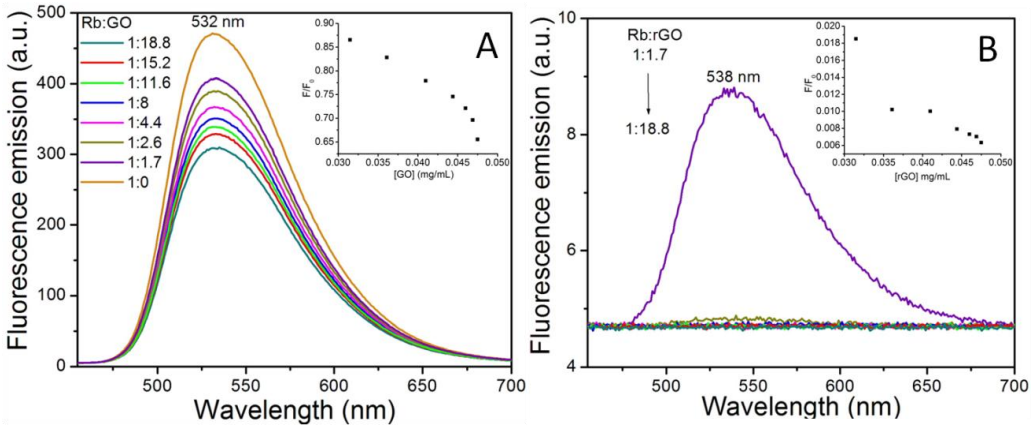

Fig. 4-1 *Fluorescence spectra of pristine Rb ($0.5x10^{-4}$M) and of the same Rb concentration in the presence of different concentrations of GO (A) and rGO (B). Insets show the F/F_0 plots against [GO] (A) and [rGO] (B). The bands widths for excitation and emission were 1 and 5 nm respectively.*

The fluorescence lifetime values are presented in the table below and predict the formation of Rb-rGO complex, rationalized by the apparition of multi-exponential decay in the case of Rb-rGO.

Samples/ χ^2	Fractional amplitude of intensity (%)/ amplitude (kCnts)	Fluorescence lifetime τ (ns)/ average lifetime < τ>
Rb χ^2=1.017	A1=100 (10.136±0.006)	τ1=4.755±0.004
Rb-GO (1:1.7) χ^2=1.058	A1=100 (9.860±0.007)	τ1=4.737±0.004
Rb-GO (1:18.8) χ^2=1.075	A1=100 (9.666±0.004)	τ1=4.711±0.002
Rb-rGO (1:1.7) χ^2=1.027	A1=97.8 A2=2.2 (A1+A2=9.63±0.018)	τ1=4.286±0.005 τ2=1.356±0.000 < τ>=4.21
Rb-rGO (1:18.8) χ^2=1.020	A1=86.5 A2=13.5 (A1+A2=2.824 ±0.014)	τ1=4.473±0.007 τ2=1.356±0.000 <τ>=4.05

Table 4-2 *Fluorescence lifetime values and corresponding fractional amplitude of intensity for Rb (at pH~10.3) and Rb-GO/rGO solutions, at the lowest and highest [GO] and [rGO].*

Raman characterization of Rb-GO/rGO

Raman measurements in Rb-GO/rGO solution confirms the strong fluorescence quenching induce by rGO in Rb. In the case of pristine Rb there are no distinguishable Raman peaks because of the strong fluorescence background. This background is diminished in case of Rb – GO, and disappears in almost all Rb-rGO samples.

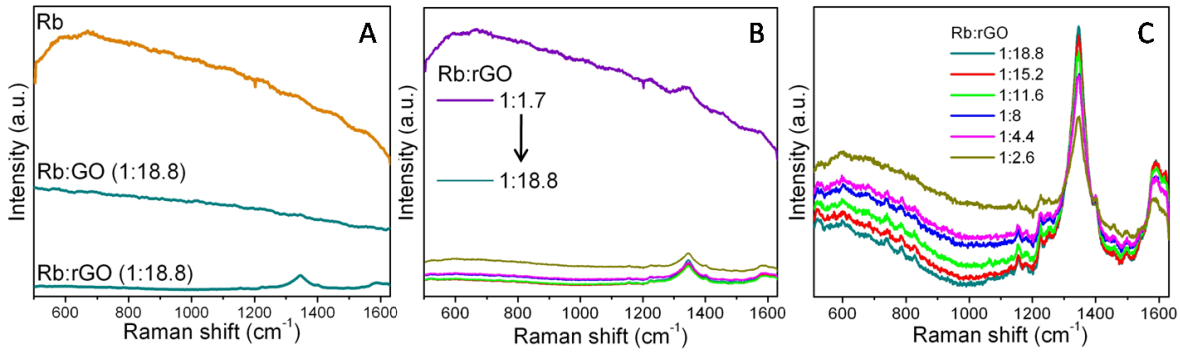

Fig. 4-3 *Raman spectra of Rb solution (orange), Rb-GO/rGO at 1:18.8 ratios (A); Rb-rGO at ratios from 1:1.7 to 1:18.8 (B); Rb-rGO at different ratios starting from 1:2.6 to 1:18.8.*

4.4.2 Monitoring the interactions and riboflavin induced fluorescence changes in graphene oxide and reduced graphene oxide

The samples obtained after centrifugation and filtering are further considered as GO – Rb (S) and rGO – Rb (S) 1…7, which denotes the initially higher and lower GO/rGO concentration.

UV-Vis absorption and steady - state fluorescence features of rGO/GO-Rb(S).

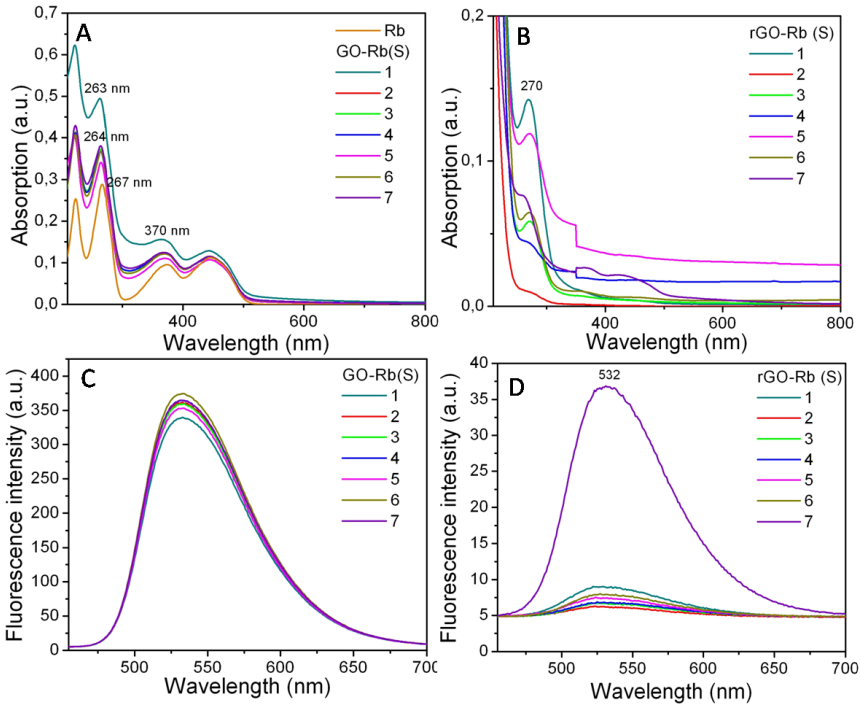

Fig. 4-4 *UV-Vis absorption spectra of (A) Rb solution and GO-Rb(S); and (B) rGO-Rb(S) at different initial (before filtering) concentration of GO and rGO. Fluorescence spectra of (C) GO-Rb(S), and (D) rGO-Rb(S) at λexc=445 nm. Bands widths for excitation and emission were 1 and 5 nm respectively.*

UV-Vis and fluorescence spectra of GO – Rb (S) show no significant changes after separation. In case of rGO – Rb (S), the UV – Vis spectra show no Rb characteristic features, while Rb fluorescence is weak.

The excitation at 375 nm of rGO – Rb (S) comprises the emission of rGO, as is seen in **Fig. 4-5** (400 – 500 nm region). The fluorescence intensity of rGO increases with decrease in the initial rGO concentration in rGO - Rb, suggesting the concentration-dependent complex formation between rGO and Rb. For comparison, the rGO (S) spectrum is showed (black line) and it shows extremely low fluorescence intensity as

compared to rGO – Rb (S). In GO – Rb (S) there are no fluorescence features in 400 – 500 nm range.

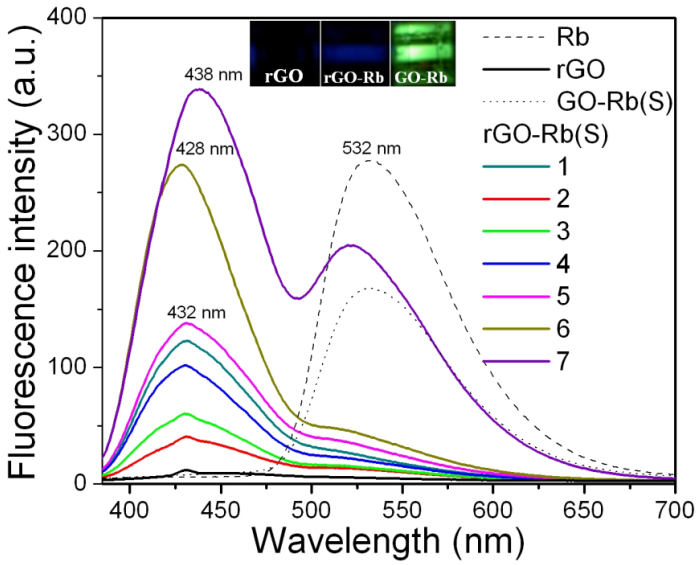

Fig. 4-5 *Fluorescence emission spectra of different rGO-Rb (S), GO-Rb (S), Rb and rGO pristine solutions at λexc=375 nm. Inset are showed optical images of rGO (S), rGO-Rb (S) and GO-Rb (S) solutions, at 375 nm excitation.*

In order to confirm whether the blue fluorescence pertains to graphene, one of the rGO – Rb sample was excited at different excitations wavelength, since in graphene the emission is excitation dependent. The below fluorescence spectra confirm that the peak in the blue region is from rGO.

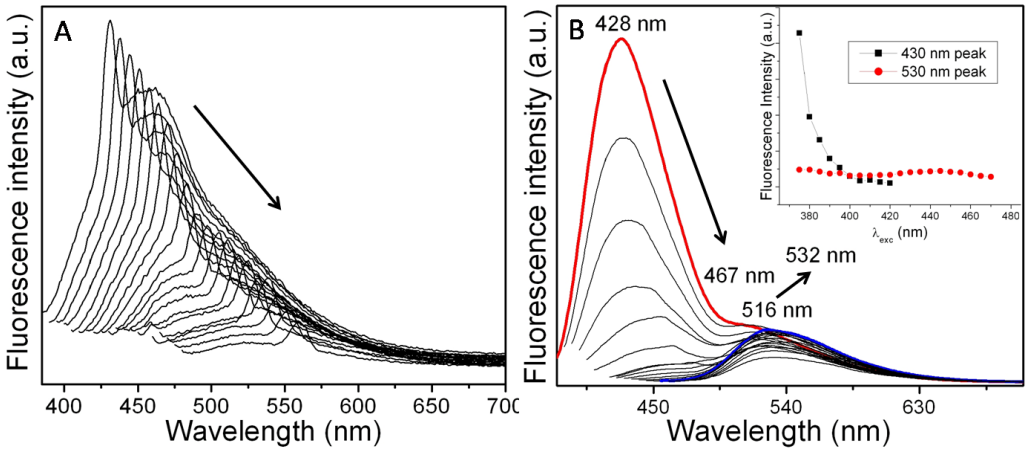

Fig. 4-6 *Fluorescence spectra of rGO (S) (A) and rGO-Rb(S) 6 (B) recorded at different λexc, from 375 to 470 nm, with a variation of 5 nm between two subsequent excitations.*

TRF (Time Resolved Fluorescence) measurements

In the table below are presented the fluorescence lifetime values for different rGO – based samples. The excitation at different wavelength allows the lifetimes values assignation, with the longer component having the higher contribution in 500 – 700 nm range, and the shorter one – in blue range. The increase in average life values in rGO – Rb (S) as compared to pristine rGO, indicates on interaction between rGO and Rb and formation of more stable excited state in complexed rGO.

Samples	**λexc-375 nm**		**λexc-485 nm**	
	Fractional amplitude of intensity (%)/amplitude (kCnts)	**Fluorescence lifetime τ (ns)/average lifetime <τ>/ χ^2**	**Fractional amplitude of intensity (%)/amplitude (kCnts)**	**Fluorescence lifetime τ (ns)/average lifetime <τ>/ χ^2**
rGO	A1=5.79 A2=10.73 A3=83.48 (A1+A2+A3=3.922±0.036)	τ1=4.99±0.13 τ2=1.218±0.051 τ3=0.22±0.002 **<τ>=0.6** **χ^2=1.046**		
rGO-Rb(S) 7	A1=58.6 A2=41.4 (A1+A2=9.427±0.013)	τ1=4.725±0.000 τ2=1.362±0.004 **<τ>=3.3** **χ^2=1.070**	A1=79.2 A2=20.8 (A1+A2=3.061±0.011)	τ1=4.737±0.006 τ2=1.356±0.000 **<τ>=4** **χ^2=0.999**
rGO-Rb(S) 1	A1=52.7 A2=47.3 (A1+A2=9.494±0.072)	τ1=4.995±0.025 τ2=1.321±0.013 **<τ>=3.25** **χ^2=1.016**	A1=76.7 A2=23.3 (A1+A2=2.17±0.023)	τ1=4.997±0.019 τ2=1.356±0.000 **<τ>=4.14** **χ^2=1.005**

Table 4-7 *Fluorescence lifetime values and corresponding fractional amplitude of intensity of pristine rGO, and Rb-rGO (S) at the initially lowest and highest [rGO].*

Further, other techniques were used for comparative study between GO – Rb and rGO – Rb, aiming the understanding of the interaction between GO/rGO and Rb. The techniques include imaging techniques: Fluorescence and Differential Interference Contrast (DIC), Fluorescence Lifetime Imaging (FLIM); Atomic Force Microscopy (AFM), Raman mapping. Further, only the most relevant information is provided.

AFM, Raman imaging

The AFM analysis show that, different from flat and ~0, 7 nm thick pristine rGO (**Fig. 4-8 A**), rGO-Rb (**Fig. 4-8 B**) presents an increased surface roughness which can be

clearly seen from the height profile, with the thickness varying between ~2 nm and ~5 nm. The observed morphology should be a consequence of Rb's stacking on both sides of rGO and its probable affinity to form nanoaggregates on the rGO surface. On the other hand, the Rb attachment determines the loss of the rGO flakes planarity and the apparition of the wrinkleless. In order to confirm whether the observed entities are Rb, Raman spectroscopy was used (**Fig. 4-8 C, D, E**). Raman mapping on two different spectral regions, appertaining to Rb (green) and rGO (blue), shows similar features, relying on interaction between rGO and Rb.

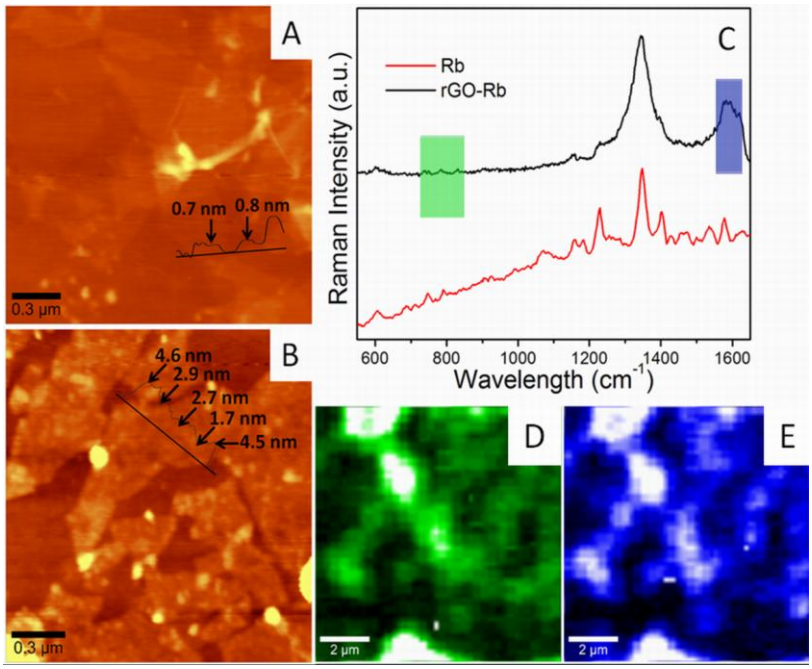

Fig. 4-8 *AFM image of rGO (A) and rGO-Rb (B); Raman spectra of Rb powder (red line) and rGO-Rb (black line) dried on glass substrate (C); Raman maps obtained from the integration of Rb peaks (732-837 cm^{-1}) (D) and rGO G band (1563-1600 cm^{-1}) (E).*

4.5 Discussions

The binding of GO/rGO with Rb. Due to the heterogeneous surface chemistry in case of GO, its binding to Rb is limited and the only possible bonds are hydrogen bonds, which are not highly favored at working pH (~10). The reduction of GO to rGO leads to the increased availability of sp^2 domains, favoring the π-π stacking interaction with Rb.

Fluorescence enhancement in rGO. There are several factors leading to low fluorescence quantum yield of rGO: extensive reduction that increases the interconnectivity between sp^2 clusters which facilitates the hopping of excitons to nonradiative recombination centers; the remained oxygen groups are deprotonated and the non- radiative electron transfer to the holes of sp^2 domains is favored; interaction with solvent molecules. Therefore, the interaction of rGO with Rb leads to: lesser conjugated system where the nonradiative hopping of the excitons will be limited (π-π interaction); inhibition of the electron donation capabilities of the oxygen groups to the holes of sp^2 domains by hydrogen bonds; limited interaction with solvent.

4.6 Conclusions

- Investigation of the interaction between graphene oxide (GO), reduced graphene oxide (rGO) with riboflavin (Rb);
- Because of the heterogeneous structure, the interaction between GO and Rb was negligible, leading to a low influence on Rb emission and no recordable complex formation;
- The more homogenous structure of rGO favored the π-π interaction with Rb and the ground-state complex formation, which leads to simultaneous fluorescence quenching in Rb and fluorescence enhancement in rGO;
- The presented results are a good start towards designing of graphene-based hybrids with tunable optical properties, of importance in optical applications.

5. Fabrication of Graphene Oxide, Carbon Nanotubes and Graphene Oxide – Carbon Nanotubes thin films

Abstract

This chapter contains the results achieved during the PhD research stage at Manchester Centre for Mesoscience & Nanotechnology (CMN), the University of Manchester. It comprises the deposition of solution - based single walled carbon nanotubes (SWCNTs), graphene oxide (GO) and hybrid GO-SWNTs films for the future fabrication of field effect transistors (FETs) characterized by scalability, low cost production and high performance.

5.1 Materials and methods

5.1.1 Materials

Single walled carbon nanotubes: metallic (MCNTs – 0.01mg/mL), semiconducting (SCNTs – 0.01 mg/mL) and unsorted (SWNTs – 0.25), dispersed in a mixture of surfactant – water. *Graphene oxide*: 3 type, different by size, surface chemistry and solvent; GO1 – lateral dimension 400nm- 1.5 um, in water; GO2 – 50 – 400 nm, in water; GO3 – 200-500 nm, more hydrophobic (reduced), in acetonitrile.

5.1.2 Deposition techniques

The methods used for the film depositions were the *dip coating* and *spin coating* techniques. Both methods were first tested on particular solution and the choice of one or another method for each of the solutions was made mainly in function of solution concentration. Particularly, the dip coating technique showed to be more suitable for low-concentrated solutions (*i.e.* MCNTs and SCNTs), while the spin coating technique gave better results on more concentrated suspensions (*e.g.* SWNTs) where dip-coating failed.

5.1.3 Substrates preparation

The films deposition was done on Si/SiO2 substrates, cut in ~1.5 cm pieces, cleaned by subsequent sonication in acetone, DI water and isopropanol, dried in N_2 flow, and treated in O_2 plasma atmosphere.

5.2 Characterization technique

In order to avoid the films contamination, the films were characterized by AFM, Veeco Dimension 3100 model, operating in Tapping Mode.

5.3 Results and discussions

5.3.1 Singe walled carbon nanotubes films

The most efficient method for the deposition of MCNT and SCNTs was dip coating, with Z – speed of 2mm/min, by heating the solution during coating. For SWNTs, the most efficient method was spin coating, operating at 1000 rpm.

In this section, several practical examples showing the importance of O_2 plasma substrate treatment are provided. It is also showed the importance of curing step after each deposition. These consideration are important in deposition of high uniform films.

5.3.2 Graphene oxide films

The most appropriate method for deposition of GO films was spin coating, operating at 400 rpm in case of GO1 and GO2, and 900 rpm – GO3 (bwGO). In the case of GO3 the deposition was difficult due to the nature of the solvent, leading to big aggregates and non-uniform deposition. The deposition was improved by mixing GO3 with DI water. In case of GO1 and GO3 the deposition showed to be poor reproductive.

5.3.3 Hybrid films

Hybrids films deposition was done by deposition of CNTs (3 types) on GO films (GO1, 2, 3), following the previously used parameters.

5.4 Examples of fabricated on films devices

In this section only several examples of fabricated on films devices are provided, with the main issues which can appear during device fabrication on films: broken electrodes, incomplete removal of photoresist and film removal.

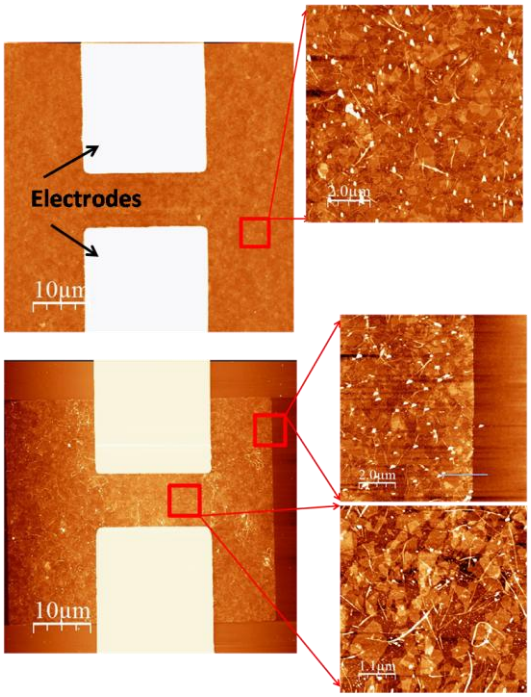

Fig. 5-1 *AFM image of an area comprising two electrodes of the device: before GO1-MCNTs film etching (top) and after successful etching (bottom).*

5.5 Conclusions

- The films deposition is affected by many parameters, like: sample concentration, solvent, the nature of deposited material;
- Several universal factors important in the film deposition process were identified and explained;
- In spite of poor reproducibility of some samples, more exemplars of the same type of uniform and thin films were obtained, suitable for further use in device fabrication.

6. Final conclusions and future perspectives

Conclusions

- Developing of a new and green method for fabrication of reduced graphene oxide – Au nanoparticles hybrids with tunable surface "decoration", enable for efficient SERS detection.
- The improvement of optical properties, *i.e.* fluorescence, of reduced graphene oxide by easy way of non-covalent functionalization with riboflavin.
- The successful solution based deposition of graphene oxide, carbon nanotubes and graphene oxide – carbon nanotubes thin films, enable for the fabrication of FETs.

Future perspectives

- To design multifunctional graphene – based platforms (*i.e.* graphene – polymer – AuNP – fluorophore) enable for sensitive SERS and fluorescence – based detection, bio-imaging, photothermal therapy, and photodynamic therapy.

List of publications and conferences

Related to Thesis (ISI)

1. **Maria Iliut**, Ana- Maria Gabudean, Cosmin Leordean, Timea Simon, Cristian-Mihail Teodorescu, Simion Astilean, *Riboflavin enhanced fluorescence of highly reduced graphene oxide*, **Chem. Phys. Lett**., 2013, 586, 127–131. (IF = 2.145)

2. **Maria Iliut**, Cosmin Leordean, Valentin Canpean, Cristian-Mihail Teodorescu, Simion Astilean, *A new green, ascorbic acid-assisted method for versatile synthesis of Au–graphene hybrids as efficient surface-enhanced Raman scattering platforms*, **J. Mater. Chem. C**, 2013, 1, 4094–4104. (IF = 6.101)

Unrelated to Thesis (ISI, BDI)

1. **Maria Iliut**, Monica Iosin, Simion Astilean, *Monitoring the effects of ultraviolet and visible light on Rb and vitamin A in milk*, EEMJ, 2012, Accepted. (IF=1.117)

2. **Maria Iliut**, Monica Focsan, Simion Astilean, *Monitoring the effects of temperature on milk by fluorescence spectroscopy of riboflavin and vitamin A*, Studia UBB Physica, 2011, LVI, 1, 17. (BDI)

Conferences

1. **Maria Iliut**, Cosmin Leordean, Valentin Canpean, Simion Astilean, *A green approach to the synthesis of graphene oxide/reduced graphene oxide-gold nanoparticles hybrids*, **EUCMOS**- European Congress on Molecular Spectroscopy- 26-31 August, 2012, Cluj-Napoca, Romania

2. **Maria Iliut**, Cosmin Leordean, Valentin Canpean, Simion Astilean, *A new green, ascorbic acid-assisted method for versatile synthesis of Au-graphene hybrids as efficient surface-enhanced Raman scattering platforms*, **Graphene Nanophotonics** - 3-8 March, 2013, Benasque, Spain.

Acknowledgements

First, I want to express my deep gratefulness to my scientific advisor, Prof. Simion Astilean for his lab and resources, for his valuable guidance during all these years, and for challenging research topic, which helped me to explore my potential and to define my research direction.

I would like to acknowledge all the members of my thesis committee for accepting to evaluate my work.

The pleasant time spent in the lab would not be such a pleasant without my colleagues from Nanobiophotonics Center, which I would like to thank for their help, suggestions and friendship.

I would also like to acknowledge all people who helped me with measurements and made this work better: Cristian Teodorescu for beautiful XPS graphs, Gabriel Katona for TEMs, Oana Ponta and Adriana Vulpoi for TEM, SEM, XRD, FTIRs, Mircea Puia for FTIRs, Lucian Barbu – Tudoran for first TEM images with my graphene.

I want to express my gratefulness to Kostya Novoselov who gave me the opportunity to spend six months in the "Big Graphene House" at Manchester University, and to Aravind Vijayaraghavan for supervising me there. It was a big pleasure and honor to be there, surrounded by graphene pioneers – modest and friendly people, to participate every Friday at "graphene meeting", and to see their presentations.

There are no words to express my deep love and gratitude to my family, which supported me in every moment of my life. Special thanks to my mom who took care of my children when I couldn't do that; to my husband for his love, patience and encouragements; to my children for their unconditional love, for waiting me all the time and for shining all my grey days

This work was supported by Sectoral Operational Programme for Human Resources Development 2007–2013, co-financed by the European Social Fund, under the project number POSDRU/107/1.5/S/76841 with the title" Modern Doctoral Studies: Internationalization and Inter- disciplinarity ".